The Applications of Laser 3D Printing in Biofabrication

激光 3D 打印在生物制造中的应用

Cijun Shuai , Chengde Gao ,
Pei Feng , Shuping Peng .

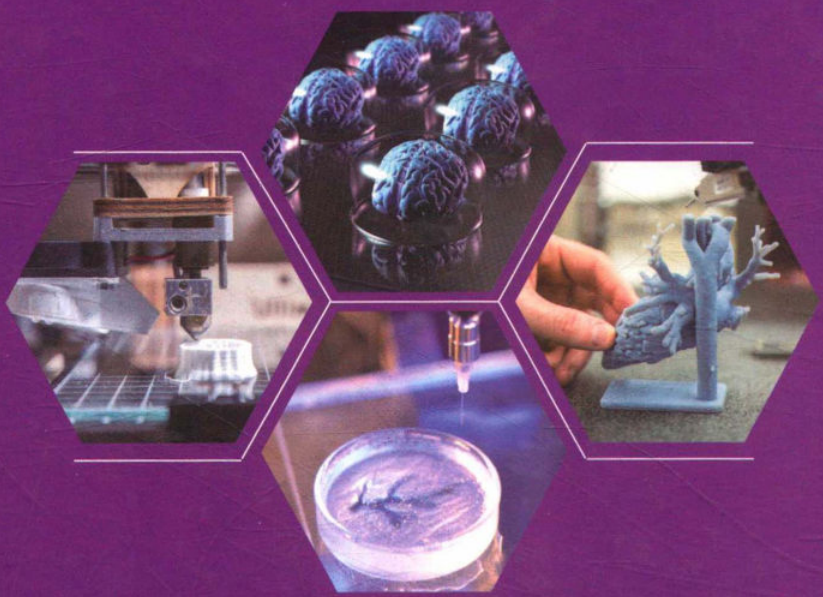

西安交通大学出版社
XI'AN JIAOTONG UNIVERSITY PRESS

The applications of laser 3D printing in biofabrication

激光3D打印在生物制造中的应用

Cijun Shuai , Chengde Gao ,

Pei Feng , Shuping Peng .

西安交通大学出版社
XI'AN JIAOTONG UNIVERSITY PRESS

图书在版编目（CIP）数据

激光3D打印在生物制造中的应用：The applications of laser 3D printing in biofabrication/帅词俊等著. —西安：西安交通大学出版社，2018.2

ISBN 978-7-5693-0444-2

Ⅰ.①激… Ⅱ.①帅… Ⅲ.①立体印刷—印刷术—应用—生物材料 Ⅳ.①Q81②TS853

中国版本图书馆CIP数据核字（2018）第033703号

书　　名　The applications of laser 3D printing in biofabrication
　　激光3D打印在生物制造中的应用
著　　者　帅词俊　高成德　冯　佩　彭淑平
责任编辑　魏　杰　贺彦峰

出版发行　西安交通大学出版社
　　（西安市兴庆南路10号　邮政编码710049）
网　　址　http://www.xjtupress.com
电　　话　（029）82668357　82667874（发行中心）
　　（029）82668315（总编办）
传　　真　（029）82668280
印　　刷　长沙市宏发印刷有限公司

开　　本　710mm×1000mm　1/16　印张 23.5　字数 427千字
版次印次　2018年2月第1版　2018年3月第1次印刷
书　　号　ISBN 978-7-5693-0444-2
定　　价　148.00元

读者购书、书店添货、如发现印装质量问题，请与本社发行中心联系、调换。

Forward

It has long been one dream of mankind to repair or reconstruct the defective tissues/organs by using biomedical implants, which have similar shape, structure and function to the natural tissues/organs. As the world's most populous country, China has entered the aging society since the end of the 20th century, and is expected to supplant Japan as the world's most aging country in 2030. The aged is a high-risk and vulnerable population of serious diseases and accidental injuries because of the decline of physiological function, weak control over environment and the phenomenon of "empty nest". As a result, tissue/organ defects are growing rapidly and there has been an ever-increasing demand for biomedical implants. In order to repair the defective tissues/organs, a biomedical implant should not only mimic the material characteristics and gradient structure of the defective sites, but also have sufficient mechanical properties to support cells and withstand complex stresses in the physiological environment. Meanwhile, the implant should possess controllable degradation rate and favorable osteoinductivity. These complex structures, harsh performance and individual differences put forward great challenges for the fabrication methods of biomedical implants. So far, biomedical implants are fabricated mainly by forging, casting and machining, which requires not only complex molds but also high cost for single-piece production. More importantly, traditional fabrication methods are difficult to obtain the gradient structure and performance of implants. Therefore, it has become a huge challenge to manufacture personalized biomedical implants for the repair and regeneration of defective tissues/organs.

In recent years, laser 3D printing, as a typical additive manufacturing technology, has provided a novel strategy for the fabrication of biomedical implants. It fabricates three-dimensional parts based on digital models and layer by layer principle, which enables not only the fabrication of complex shape and internal structure but also rapid fabrication without molds. Therefore, it has significant advantages in

the fabrication of small batch implants with personalized and complex structure. At present, although many developments have been achieved in the laser 3D printing of biomedical implants, there are still many difficulties from the clinical application. On one hand, the implant materials should fulfill not only the characteristics (such as biocompatibility, mechanical properties and biodegradability, etc.) for tissue/organ repair but also the requirements for laser 3D printing, as the tissues and organs are composed of a variety of heterogeneous materials. Current studies mainly focus on exploring the laser 3D printing process of a single type of biomaterial, which, however, can hardly meet the multiple requirements of tissue/organ repair. Some research attempt to fabricate multi-material implants by printing different types of biomaterials at the same time. However, it is difficult to obtain good interfacial bonding between different types of biomaterials due to their significant differences in physicochemical properties and processability. As a result, the performance of fabricated implants are far from expected. Therefore, there is still a long way to go to explore the laser 3D printing process for heterogeneous biomaterials in order to fabricate suitable biomedical implants.

To accelerate the development of biomedical and 3D printing industries: advanced medical equipment and biomedical materials and advanced manufacturing (including laser 3D printing) technology have been proposed as the priority themes in the National Medium and Long-term Science and Technology Development Plan. To speed up the developments of additive manufacturing industry, the National Growth and Development Industry Promotion Project (2015—2016) has been established by the Ministry of Industry and Information Technology, the Development and Reform Commission and the Ministry of Finance have formulated. Moreover, many foundations (including the National Natural Science Foundation of China) are also giving great supports for the studies on biomedical implants and additive manufacturing. It is foreseeable that the research on laser 3D printing of biomedical implants will be an extremely important component of the future healthcare industry and become a hot spot of interdisciplinary research worldwide in the next few decades. This book summarizes the advantages and disadvantages of different types of biomaterials as biomedical implants by analyzing the physiochemical properties, the formability in laser 3D printing, and biomechanical properties of bioceramics, polymers and biomedical metals. Moreover, a series of methods, including

second-phase reinforcing by low-dimensional nanomaterials or oxides, alloying and liquid-phase sintering, etc., are proposed to compensate or overcome their disadvantages. Afterwards, the laser 3D printing process of multi-type biomaterials is explored, and the interfacial interactions between the different types of biomaterials and the formation mechanisms of properties are revealed. Moreover, the effects of material composition and printing process on the formability and final performance of biomedical implants are systematically summarized. And the laser 3D printing principle and technology for multi-material implants are established. The book consists of the following five chapters:

Chapter I: Low-dimensional nanomaterials reinforced biomaterials by laser 3D printing

Chapter II: Oxides reinforced biomaterials by laser 3D printing

Chapter III: Alloying elements in biomedical metals by laser rapid solidification

Chapter IV: Liquid phase-assisted densification in laser 3D printing

Chapter V: Combination of different types of biomaterials by laser 3D printing

This book is supported by the following funds: (1) The Natural Science Foundation of China (51575537, 81572577, 51705540); (2) Hunan Provincial Natural Science Foundation of China (2016JJ1027); (3) The Project of Innovation-driven Plan of Central South University (2016CX023); (4) The Open-End Fund for the Valuable and Precision Instruments of Central South University; (5) The fund of the State Key Laboratory of Solidification Processing in NWPU (SKLSP201605); (6) National Postdoctoral Program for Innovative Talents (BX201700291); (7) The Project of State Key Laboratory of High Performance Complex Manufacturing, Central South University.

The authors have long been engaged in the research in biofabrication by laser 3D printing. Many contents in this book are the summary of the achievements during the authors' research work, and the research findings of the peers at home and abroad are also assimilated. During the summarization, sorting and compiling process, we have also referred to a large number of papers and works by other experts and scholars and are strongly supported by Central South University and Jiangxi University of Science and Technology. Here, we express our heartfelt thanks to the

teachers and students who have provided support and assistance for the publication of this book. This book can be used as a reference book for scientific researchers and college students. It provides the experimental means, material composition and processing data for multi-disciplinary research, such as manufacturing science, medical science, etc., thereby promoting the repair and regeneration of tissues/organs and the development of related disciplines. Due to the limited knowledge of the authors and the rapid development of science and technology, some flaws and mistakes are unavoidable in the book, and criticisms and corrections are sincerely welcomed.

CONTENTS

Chapter I Low-dimensional nanomaterials reinforced biomaterials by laser 3D printing

Nanodiamond reinforced polyvinylidene fluoride/ bioglass scaffolds for bone tissue engineering

Abstract: An interconnected porous Polyvinylidene fluoride/bioglass (PVDF/BG) scaffold was prepared by selective laser sintering. Its mechanical properties and bioactivitywere reinforced bynanodiamond. The tensile strength successfully achieved to 59.61 MPa, which increased by 23.01% when the nanodiamond content was 1 wt%. It might be because nanodiamond particles dispersed in the matrix uniformly and had a good interface bonding with the matrix. Moreover, nanodiamond enhanced the scaffold bioactivity, which was proved by the biological mineralization and cell culture experiments. The nanodiamond reinforced scaffolds might have potential application for bone tissue engineering.

Keywords: scaffolds, nanodiamond, tensile strength, bioactivity, biocompatibility

1 Introduction

Polyvinylidene fluoride (PVDF) has good biocompatibility, commendable thermal stability and excellent processability [1]. Therefore, PVDF has been used in various sections, such as tissue engineering, filtration and hydrogen production, in which the application in tissue engineering has attracted more and more attention [2-5]. However, PVDF has poor bioactivity, biodegradation and insufficient strength when it is prepared into porous scaffolds, which restrict its further application in living organisms. Bioactive glass (BG) has good bioactivity, bone-bonding property and biodegradability. Moreover, Ca and P ions release from BG can stimulate the growth, proliferation and differentiation of osteoblasts [6-8]. Recently, BG was usually used to

improve the biological properties of polymers [9-12].

Nanodiamond has attracted wide attention owing to its superior mechanical properties, biocompatibility, chemical stability and large specific surface area[13-15]. Moreover, there exist a large number of free electrons and functional groups on the surface of nanodiamond in contrast to many other carbon nanomaterials, which make its surface could be modified [16, 17]. Based on the above advantages, nanodiamond has potential application prospects in reinforcing the mechanical properties of PVDF.

The effect of nanodiamond used as reinforcement phase has been studied. Ning Cai et al. discovered that the tensile strength of the nanodiamond/Poly(lactic acid) (PLA) scaffold increased by 240% with 1 wt% nonadiamond [18]. Yury Gogotsi et al. found that 10 wt% of nanodiamond induced a 2.8-fold increase in the strain to failure and reinforced the PLLA bioactivity [19]. Yu-Jun Zhai et al. discovered that the tensile strength, tensile modulus and Vicker's hardness of the composites increased by 52.7%, 54.2% and 24.7% respectively with 0.3 wt% nanodiamond [20].

In this paper, nanodiamond and BG were used to improve the mechanical properties and the bioactivity of the scaffolds, respectively. Their microstructure and composition were researched by scanning electron microscopy (SEM) and X-ray diffraction (XRD). Besides, the bioactivity and biocompatibility were assessed with simulated body fluid (SBF) and MG-63 cell culture.

2 Experiments and Characterization

2.1 Materials

Nanodiamond (particles sizes 5-10 nm, purity 97%) was provided by Nanjing XFNANO Materials Tech Co., Ltd. 63s BG (particle size μm) was purchased from the KunShan Chinese Technology New Materials Co. Ltd. PVDF (Mw = 275, 000 g/mol, particle diameter -250 nm) was obtained from Huangjiang Huayi Plastics Material Co. Ltd.

The PVDF/BG mixed powders were prepared and the process was as follow: the PVDF and BG powders were weighed according to the certain proportion (95 wt% PVDF and 5 wt% BG), respectively. They were then added into a 30 mL beaker with

15 mL absolute ethyl alcohol. Subsequently, the solutions were processed with ultrasonic 20 min at 50 ℃ using ultrasonic cleaning device (Shanghai Kudos Ultrasonic Instrument Co., Ltd, China) for distributing the BG particles. Afterwards, in order to further dispersing, the solutions were treated with a planetary high-energy ball mill (Changsha Deco Equipment Co., Ltd, China) for 30 min at 1100 r/min. Finally, the solutions were filtered slowly. The mixed powders were obtained, and then preserved in electrothermal blowing dry box at 60 ℃. The nanodiamond powders were added into the PVDF/BG mixed powders according to the certain proportion (0.5 wt%, 1 wt%, 2 wt% and 3 wt%), and then repeated the previous process steps to obtain the final mixed powders.

2.2 Scaffolds

The scaffolds were fabricated via layer-by-layer selective laser sintering (SLS) [21, 22]. The fabrication process was as follow: The mixed powders were paved on the sintering platform and sintered with the focus laser beam. Afterwards, the sintering platform moved down with a powders layer thick. The sintering process repeated until the scaffolds were prepared completely. The processing parameters were set as follows: layer thickness 0.1-0.2 mm, spot diameter 0.8 mm, scan speed 400 mm/min and scan space 3.0 mm. The powders were removed after the sintering process and the scaffolds were cleaned with compressed air. The fabricated scaffolds used for experiments were divided into different groups.

2.3 Characterization

The tensile tests were carried out using a universal testing machine with a 100 N load cell. A free-moving wedge grip and fixed lower were used to fix the scaffolds. The speed for the tensile experiments was set at 0.5 mm/min and five scaffolds were tested for each test group. The tensile strength was obtained through data process according to the experiment data recorded. The compositions of the scaffolds before and after immersing in simulated body fluid (SBF) were analyzed by X-ray diffraction (XRD, Bruker AXS Inc., Germany) with Cu-Kα radiation. The scanning rate was set at 8 °/min and the data from 15° to 70° was recorded. The morphology of the scaffolds, bone-like apatite and cells were examined by Scanning electron microscopy (SEM, JEOL Co., Japan). The technical parameters of the SEM were set at

low-vacuum mode (2.0 nm) and 1kv accelerating voltage. In this paper, the magnification times were 20000X when observing the morphology of scaffolds and the bone-like apatite. 2000X was used to observe the morphology of the cells. All the scaffolds were coated with platinum using a sputter coater (JFC-1600, JEOL, Japan) for 120 s at 10 mA under vacuum before experiments. Chemical microanalysis was conducted with Energy dispersive spectroscopy (EDS, Oxford Inc., UK).

2.4 Bioactivity

The scaffolds were incubated in simulated body fluid (SBF) for 7, 14 and 21 days in order to evaluate their bioactivity. The SBF was prepared using the method that our research team used before [23]. The scaffolds used for the experiments were put into a 30 mL beaker with 10 mL absolute ethyl alcohol. Then, the beaker was processed with ultrasonic cleaning device for 10 min in order to clean and sterilize the scaffolds. Subsequently, the scaffolds were placed in 12-well tissue culture plates. Fresh medium were changed every second days until day 21. After immersion for different time periods, the scaffolds were removed from the medium. Afterwards, the scaffolds were immersed into deionized water to sweep inorganic ions three times. Finally, the scaffolds were dried for the subsequent experiments.

2.5 Biocompatibility

MG-63 cells were used to conduct cell culture experiments. MG-63 cells were incubated in Dulbecco's modified Eagle medium (DMEM) containing 0.1 mg/mL streptomycin, 80 units/mL penicillin, 10% fetal bovine serum (FBS) and 2 mmol/L L-glutamine. Then, they were cultured on a fully humid thermosforma at human body temperature (37 ℃) and 5% CO_2 atmosphere. Cells were passaged 4-6 times. Before the experiments, the scaffolds were sterilized with 70% ethanol for 2 h, rinsed with phosphate buffered saline (PBS) three times, and then exposed to ultraviolet light 15 min. MG-63 cell suspension was added into the scaffolds and cultured in a 12-well culture plate placed in a humid incubator at human body temperature (37 ℃) and 5% CO_2 atmosphere for 1, 3 and 5 days. The culture solution was changed every day. At predetermined time, the scaffolds were moved from the culture medium, rinsed with PBS and fixed with 3% glutaraldehyde subsequently. The scaffolds were then dehydrated with alcohols. Finally, the scaffolds were coated with platinum for

examining the cell morphology.

Cell immunofluorescence was used to evaluate the attachment and morphology of the MG-63 cells. The process was as follow: After 1, 3 and 5 days of incubation, cells were washed with PBS two times (5 min once time). Then, the cells were fastened using 4% paraformaldehyde (Sigma, St. Louis, MI, USA) for 20 min at 37 ℃ and then permeabilized with 0.2% Triton X-100 for 15 min. Afterwards, the cells were incubated overnight with anti-4D2 at 4 ℃ and washed with PBS and cultured with fluorescein isothiocyanate for 1 h at 37 ℃ the next day. Finally, the pictures were obtained by luminescence microscope.

2.6 Statistical Analysis

Results were presented as means ± standard error. The experimental data were analyzed by Origin 8.0 software. Statistical significance was evaluated with Student's t-test and $p < 0.05$.

3 Results and Discussion

3.1 Mechanical Properties

The tensile strength of the scaffolds increased with the content of nanodiamond increasing at first (Figure 1). The optimal tensile strength was 59.61 MPa when its content was 1 wt%, which increased by 23.01% compared with the scaffolds containing 0 wt% nanodiamond. However, the increasing trend of the tensile strength started to reverse when further increasing the content. The results indicated that superfluous nanodiamond decreased the tensile strength of the scaffolds.

The morphologies of the scaffolds were assessed (Figure 2). Some particles were inlayed into the matrix (Figures 2b-f). The composition of the scaffolds was analyzed with EDS (Figures 2g-i). The test areas were marked with frame and roman numbers (Ⅰ, Ⅱ and Ⅲ). In Figure 2h, the appeared peaks of Ca, P and Si indicated that the particles appeared in Figure 2b were BG. In Figure 2i, the C content increased compared with the pure PVDF, which indicated that the particles appeared in the scaffolds were nanodiamond marked with arrow (Figures 2c-f). In Figure 2e and f, the agglomerates of nanodiamond formed when the content of nanodiamond exceeded 1 wt%, which induced the decrease of tensile strength.

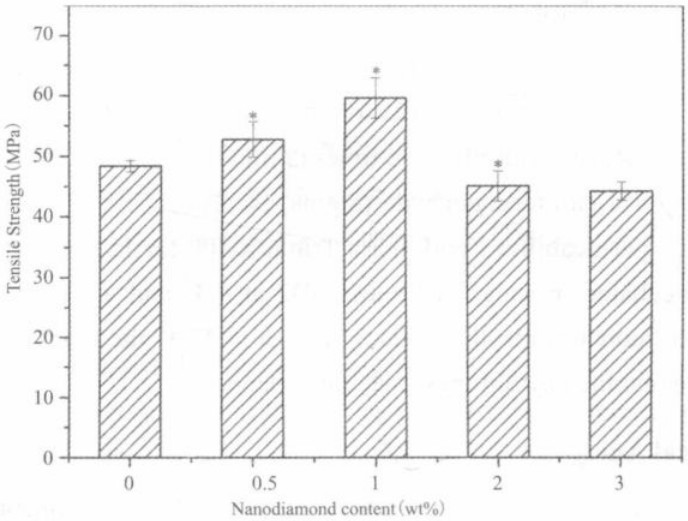

Figure 1. The tensile strength of the scaffolds containing different content of nanodiamond.

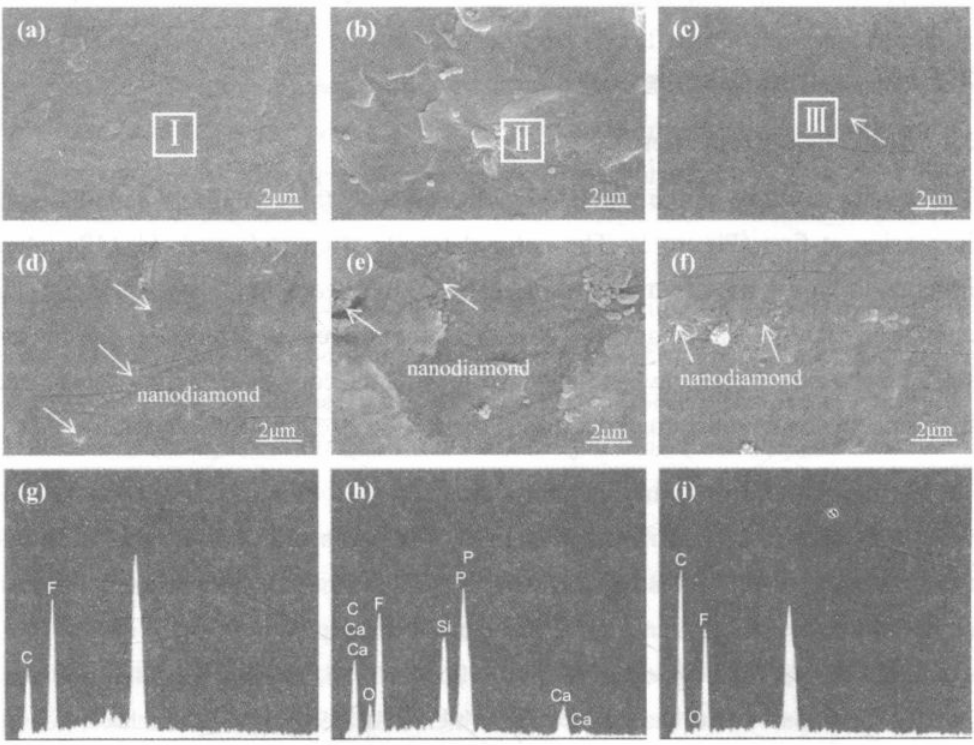

Figure 2. The surface of the scaffolds containing different content of reinforcement phase: (a) PVDF, (b) PVDF/BG, (c) 0.5 wt% nanodiamond-PVDF/BG, (d) 1 wt% nanodiamond-PVDF/BG, (e) 2 wt% nanodiamond-PVDF/BG and (f) 3 wt% nanodiamond-PVDF/BG scaffold, EDS spectrums: (g) Ⅰ, (h) Ⅱ, (i) Ⅲ.

The reasons for the reinforcement effect were the excellent mechanical properties of nanodiamond and the good interfacial adhesion between nanodiamond and PVDF matrix. While, nanoparticles could form aggregates easily during the fabrication process of mixed powders attributed to their inherent intermolecular forces and high surface energy. So the dispersion of nanoparticles was crucial for mechanical property. Although ultrasonic agitation and ball mill were used to disperse nanodiamond particles, monodispersion of nanodiamond could not be obtained. The aggregation formed during the fabrication process of mixed powders when the content of nanodiamond exceeded 1 wt%, which weakened the interface bonding. Thus, the reinforcement effect of nanodiamond was counteracted, resulting impaired mechanical properties.

3.2 Composition Analysis

The compositions of the scaffolds were analyzed by XRD (Figure 3). It could be seen that there were no obvious change between different groups. The location of characterization peaks of PVDF was not changed and its value was 18.3°, 20.0°, and 26.6° corresponding to (020), (110) and (021) respectively, which was corresponded with the literature [5]. The existent peaks demonstrated that the addition of nanodiamond and BG didn't change the location of the PVDF phase. The nanodiamond and BG were not detected. There were some reasons to illustrate the results. The one reason was that BG was noncrystalline. And the other reason was that the contents of nanodiamond and BG were too low.

3.3 Fabrication of Scaffolds

According to the results of mechanical testing, the 1 wt% nanodiamond was deemed to the optimal. So the PVDF/BG scaffolds with 1 wt% nanodiamond were fabricated via our home-made SLS system (Figure 4). The scaffold was integrity and its pores distributed evenly, which indicated that SLS could fabricate the scaffolds with customized shape. The interconnected porous structure was beneficial for the growth of cells, the formation of bone-like apatite and the transmission of nutrition and waste.

The fabricated scaffolds were used to conduct the subsequent biological experi-

ments.

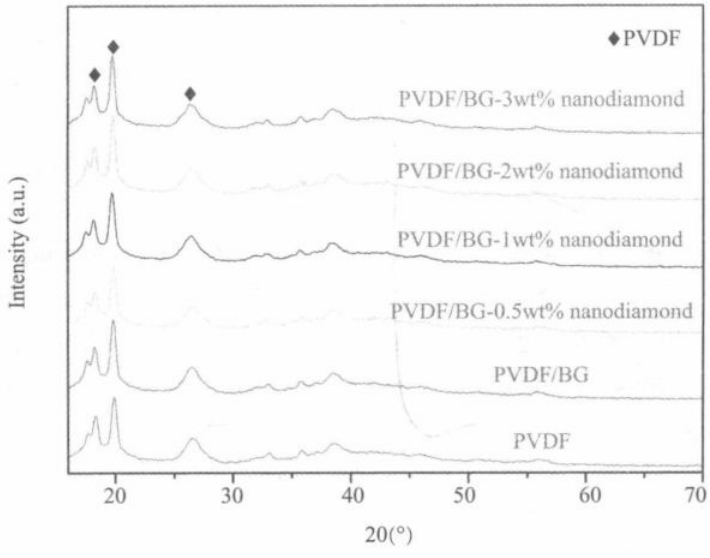

Figure 3. XRD spectrum of the scaffolds.

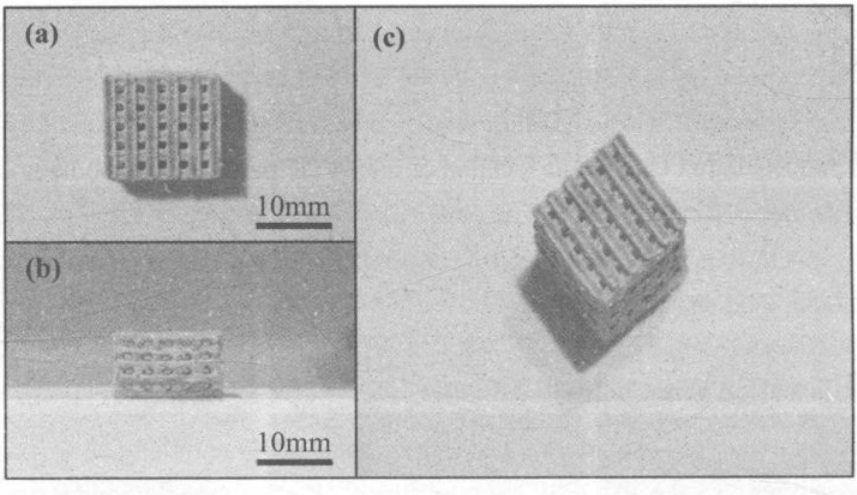

Figure 4. The PVDF/BG scaffold with 1 wt% nanodiamond prepared by SLS: (a) top view, (b) lateralview, (c) isometric view.

3.4 Biomineralization

The scaffolds were incubated in SBF for 7, 14 and 21 days respectively to evaulate the bioactivity of the scaffolds. The PVDF scaffolds were set as control. The morphology of the scaffolds after immersing in SBF was assessed (Figure 5). No deposites appeared